Lattice Dynamics of Lithium Fluoride*

G. DOLLING,† H. G. SMITH, R. M. NICKLOW, P. R. VIJAYARAGHAVAN,‡ AND M. K. WILKINSON
Solid State Division, Oak Ridge National Laboratory, Oak Ridge, Tennessee
(Received 27 October 1967)

The frequency wave-vector dispersion relation for the normal modes of vibration of Li^7F at 298°K has been measured by means of slow-neutron inelastic scattering techniques. Triple-axis crystal spectrometers at two reactor facilities at the Oak Ridge National Laboratory were employed, mostly in the "constant-Q" mode of operation. The results can be satisfactorily fitted by a seven-parameter dipole approximation model involving nearest-neighbor and second-nearest-neighbor F^--F^- short-range forces, a variable ionic charge, and the polarizability of the F^- ions only. The applicability of other force models to Li^7F is also discussed. Certain inconsistencies have been found between the slopes of the acoustic branches near $\mathbf{q}=0$ and the appropriate velocities of sound as measured by ultrasonic techniques. It is believed that these arise from anharmonic effects. The frequency distribution of the normal modes has been computed with high precision from the best-fit dipole approximation model, together with related quantities such as the lattice heat capacity, entropy, and Debye-Waller factors for each ion. Combined (two-phonon) density-of-states functions have also been calculated; comparisons are made between these one- and two-phonon distribution functions and certain features observed in optical and infrared absorption experiments on LiF.

I. INTRODUCTION

THE physical properties of lithium fluoride, LiF, have been extensively studied for many years. Thus its crystal structure (the face-centered cubic NaCl structure), heat capacity, elastic constants, high- and low-frequency dielectric constants, and many other properties, have been determined, and it is of great interest and importance to try to correlate all such properties as far as possible in terms of a basic theory of the interionic forces and ionic polarizabilities for this material. This problem may be approached from either a theoretical or an experimental viewpoint; here we are primarily concerned with a presentation of experimental measurements of the phonon dispersion curves and their analysis in terms of semiempirical interionic force models, and the use of these models to compute various physical properties. It is hoped that this will provide incentive for further work on the fundamental theory of the dynamics of alkali halides in general.

The technique of coherent inelastic scattering of slow neutrons[1] by single crystals is one of the most direct methods of obtaining information about interatomic forces in solids. A large number of relatively simple solids have been investigated in this way during the past several years, and several reviews of this subject are available.[2,3] The alkali halides NaI,[4] KBr,[5] NaF,[6] KI,[7] and NaCl[8] are among those already studied. The present experiments have been carried out at 298°K with a single-crystal specimen of lithium fluoride containing 99.993% of the Li^7 isotope, which has a much lower neutron absorption cross section than Li^6. Subsequent papers will describe experiments on Li^7F at lower temperatures and also on Li^6F and mixtures of the two, in order to study isotope effects.

Several superficially different theoretical treatments exist[4,9,10] of the crystal dynamics of alkali halides in terms of harmonic, two-body forces, and the relation between these treatments (actually very close) is well known.[11] A more fundamental theory in which the (many-body) interatomic forces are treated quantum mechanically from first principles has been developed by Löwdin,[12] and by Lundquist,[13] but the greater difficulty of this approach has so far prevented a satisfactory calculation of the dynamical properties.

In Sec. II we briefly summarize the theory underlying the inelastic neutron-scattering method, describe the type of spectrometer employed, and present the experimental results. The analysis of these results in terms of the dipole approximation model[4,11] is given in Sec. III, together with various calculations based on this model. The results are also analyzed in terms of the so-called "breathing shell model" proposed by Schröder[14] and Nusslein and Schröder,[15] which is a simple extension of the dipole approximation model to allow for the compressibility of the valence electron "shell" of the fluoride ion. The applicability of this breathing shell model to the case of LiF and other alkali halides is discussed.

* Research sponsored by the U. S. Atomic Energy Commission under contract with the Union Carbide Corporation.

† Guest scientist from Chalk River Nuclear Laboratories, Chalk River, Ont., Canada (now returned).

‡ Guest scientist from Bhabha Atomic Research Centre, Trombay, Bombay, India.

[1] G. Placzek and L. Van Hove, Phys. Rev. **93**, 1207 (1954).

[2] W. Cochran, Rept. Progr. Phys. **26**, 1 (1963).

[3] G. Dolling and A. D. B. Woods, in *Thermal Neutral Scattering*, edited by P. A. Egelstaff (Academic Press Inc., New York, 1965).

[4] A. D. B. Woods, W. Cochran, and B. N. Brockhouse, Phys. Rev. **119**, 980 (1960).

[5] A. D. B. Woods, B. N. Brockhouse, R. A. Cowley, and W. Cochran, Phys. Rev. **131**, 1025 (1963).

[6] W. J. L. Buyers, Phys. Rev. **153**, 923 (1967).

[7] G. Dolling, R. A. Cowley, C. Schittenhelm, and I. M. Thorson, Phys. Rev. **147**, 577 (1966).

[8] R. E. Schmunk, Bull. Am. Phys. Soc. **12**, 281 (1967).

[9] K. B. Tolpygo, Fiz. Tverd. Tela **3**, 943 (1961) [English transl.: Soviet Phys.—Solid State **3**, 685 (1961)].

[10] A. M. Karo and J. R. Hardy, Phys. Rev. **129**, 2024 (1963).

[11] R. A. Cowley, W. Cochran, B. N. Brockhouse, and A. D. B. Woods, Phys. Rev. **131**, 1030 (1963).

[12] P. O. Löwdin, *A Theoretical Investigation into Some Properties of Ionic Crystals* (Almqvist and Wiksells, boktrycheri AB, Uppsala, Sweden, 1948).

[13] S. O. Lundquist, Arkiv Fysik **9**, 435 (1955); **12**, 263 (1957).

[14] U. Schröder, Solid State Commun. **4**, 347 (1966).

[15] V. Nüsslein and U. Schröder, Phys. Status Solidi **21**, 309 (1967).

The Debye-Waller factors for the Li^+ and F^- ions are calculated in the harmonic approximation, and an insight into the actual motions of the two ions is thereby obtained. The locations of critical points[16] in both the frequency distribution $g(\nu)$ for the normal modes of vibration (frequency ν), and also a combined (two-phonon) density of states, are determined from the dipole approximation model. The former is of interest, for example, in the study of sidebands in the absorption spectra of defects (F centers, U centers) in LiF, while the latter will facilitate the interpretation of the two-phonon infrared absorption spectrum and of second-order Raman scattering experiments.

The velocity of sound in a particular direction in a crystal may be calculated in the harmonic approximation from the appropriate elastic constants. In a real anharmonic crystal, however, the sound propagation will vary in a complicated way with the vibration frequency. Recent calculations of these effects for KBr[17] have shown that discrepancies of the order of several percent may exist between the sound velocity at ultrasonic frequencies ($\sim 10^9$–10^{10} cps) and at the very high frequencies ($\sim 10^{12}$ cps) of the phonons studied in inelastic neutron-scattering experiments. Preliminary attempts to observe these discrepancies in Li^7F will be described below.

II. EXPERIMENTAL METHOD AND RESULTS

A. Theoretical Basis of Method

Coherent neutron-scattering processes from a single-crystal specimen in which one phonon of the lattice vibrations is either created or annihilated are governed by two conservation conditions[1]:

$$\mathbf{k}_0-\mathbf{k}'=\mathbf{Q}=2\pi\boldsymbol{\tau}+\mathbf{q}, \tag{1}$$

$$E_0-E'=\pm h\nu, \tag{2}$$

where $\mathbf{k}_0$ ($\mathbf{k}'$) and E (E') are the wave vector and energy of the incident (scattered) neutrons, $\mathbf{Q}$ is the momentum transfer vector, and $\boldsymbol{\tau}$ is a vector of the reciprocal lattice of the crystal. In the harmonic approximation, there is a well-defined *dispersion relation*, $\nu=\nu_j(\mathbf{q})$, between the frequency ν and the wave vector $\mathbf{q}$ for the normal modes of vibration of the crystal; j denotes the polarization of the mode. Thus the energy distribution of the scattered neutrons consists, in this approximation, of a small number of δ-function peaks at which Eqs. (1) and (2) may be satisfied simultaneously with the dispersion relation. In practice, these peaks are broadened partly by instrumental resolution and partly by anharmonic effects[18,19] which limit the lifetime of the normal modes.

[16] L. Van Hove, Phys. Rev. **89**, 1189 (1953).
[17] R. A. Cowley, Proc. Phys. Soc. (London) **90**, 1127 (1967).
[18] A. A. Maradudin and A. E. Fein, Phys. Rev. **128**, 2589 (1962).
[19] R. A. Cowley, Advan. Phys. **12**, 421 (1963).

The intensity of coherent one-phonon scattering of slow neutrons, under the conditions of a "constant-$\mathbf{Q}$" scan over the jth mode, is given by[20]

$$I_j=\frac{h}{4\pi}\frac{k'}{k_0}(n_j+\tfrac{1}{2}\pm\tfrac{1}{2})\left|\sum_s \xi_{sj}\cdot\mathbf{Q} \times\exp(2\pi i\boldsymbol{\tau}\cdot\mathbf{r}_s)b_s/[\exp(W_s)(\nu_j m_s)^{1/2}]\right|^2, \tag{3}$$

where $n_j=[\exp(h\nu_j/k_BT)-1]^{-1}$ and the $+$ ($-$) sign refers to neutron energy loss (gain), ξ_{sj} is the normalized eigenvector of the sth ion in the unit cell in the jth mode of vibration, and b_s, W_s, $\mathbf{r}_s$, and m_s are the coherent scattering length, Debye-Waller factor, position vector within the unit cell, and mass of the sth ion, respectively. The summation is over all s ions in the primitive unit cell.

As will be seen later, the Debye-Waller factors W_s for the Li^+ and F^- ions are quite different, but at room temperature and for typical values of the momentum transfer vector $\mathbf{Q}$, their magnitudes are rather small and so e^{-W_s} is close to unity in both cases and may therefore be omitted from the equations. For wave vectors $\mathbf{q}$ along a symmetry direction, the vectors ξ_{sj} for each s are parallel and may be expressed as a product of a unit vector $\hat{\xi}_j$ and their magnitudes ξ_{sj}. It is then convenient to define a reduced inelastic structure factor g_j^2:

$$g_j^2=(\hat{\xi}_j\cdot\mathbf{Q})^2\left|\sum_s \xi_{sj}\exp(2\pi i\boldsymbol{\tau}\cdot\mathbf{r}_s)b_s/(\nu_j m_s)^{1/2}\right|^2 =\frac{(\hat{\xi}_j\cdot\mathbf{Q})^2 b_1^2}{m_1\nu_j}\frac{[1+\mu b_2U_2/b_1U_1]^2}{[1+m_2U_2^2/m_1U_1^2]},$$

where $U_s=\xi_{sj}/m_s^{1/2}$, and $\mu=+1$ (-1) if the reciprocal lattice vector involved [see Eq. (1)] has even (odd) indices.

This inelastic structure factor may be calculated for any mode of vibration if we know the appropriate eigenvectors ξ_{sj}. These may be obtained from a theoretical model, such as the dipole approximation model to be discussed in Sec. III.

B. Specimen

The Li^7F specimen (99.993% Li^7) was cut from a 500-g single-crystal ingot furnished by R. Thoma of the Oak Ridge National Laboratory. The cut crystal weighed 90 g and was in the shape of an elliptical disk 4.5 cm $\times$4.8 cm $\times$2.0 cm thick. Its mosaic spread was 0.3°.

C. Triple-Axis Crystal Spectrometers

The bulk of the experiments were performed by means of a triple-axis crystal spectrometer mounted at facility HN-4 of the Oak Ridge Research Reactor (ORR). The high-frequency longitudinal optic modes and a selection of other modes were subsequently studied with the help

[20] I. Waller and P. O. Fröman, Arkiv Fysik **4**, 183 (1952).

of a new spectrometer at facility HB-3 of the High Flux Isotope Reactor (HFIR) at Oak Ridge.

The ORR spectrometer is shown schematically in Fig. 1. Only a brief description of it will be given here, since a more detailed account will be published elsewhere.[21] In principle it is very similar to the crystal spectrometer developed by Brockhouse,[22] but there are a number of practical differences. Thus, in the experiments at the ORR reactor, single crystals of beryllium (having mosaic spreads approximately 0.25°) were used as monochromator and analyzer crystals (see Fig. 1). An incident neutron beam can be obtained from any of four beam ports at various values of the angle $2\theta_M(=11°, 22°, 34°$, and $45°)$. With aid of the various reflecting planes of Be and these four $2\theta_M$ values, a wide variety of neutron energies E_0 can be obtained. Values of E_0 used in these experiments were 0.0466, 0.0798, and 0.1071 eV. In a typical scan, the energy E_0 is kept fixed and the analyzer angle $2\theta_A$ (and hence E') is varied over a suitable range. The scattering angle ϕ and specimen orientation ψ are simultaneously adjusted so as to maintain the neutron momentum transfer ($\hbar\mathbf{Q}$) constant at some preselected value. Most of the experiments were performed in this manner, though in some cases the neutron energy transfer was kept fixed while $\mathbf{Q}$ was allowed to vary along a preselected straight line in reciprocal space. The results of three "constant-$\mathbf{Q}$" type scans are shown in Fig. 2. The pair on the left was obtained with the ORR spectrometer, while the right-hand group was observed at the HFIR. In each case, the scattered neutron intensity (which is normalized to a given number of incident neutrons) shows a peak at an energy transfer for which Eqs. (1) and (2) are satisfied, and the peak position thus gives one point on the dispersion relation $\nu(\mathbf{q})$ by straightforward application of these equations. The observed peak positions have been corrected where necessary for the effects of (a) sloping background, (b)

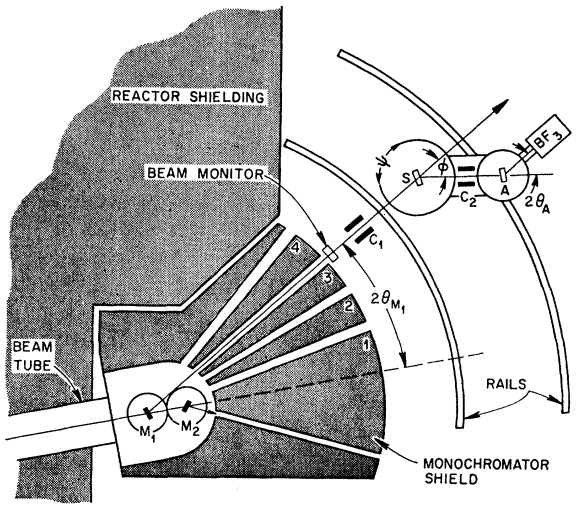

FIG. 1. Schematic diagram of the triple-axis crystal spectrometer mounted at the Oak Ridge Research Reactor (ORR).

variation of neutron-scattering cross section across the phonon energy spread, and (c) vertical divergence of the collimation system and crystal mosaic spreads. This last correction is particularly important for the long-wavelength longitudinal acoustic (LA) modes which will be discussed below.

As stated above, some experiments were performed by means of the HFIR triple-axis spectrometer; the much improved signal-to-noise ratio obtainable at the HFIR, as compared to the ORR reactor, made the observation of neutron-scattering processes involving high-frequency LO phonons considerably easier at this new reactor. The HFIR spectrometer, shown schematically in Fig. 3, differs from its predecessor at the ORR reactor in several respects, the two most important of which are (a) the monochromator crystal and its shielding may be continuously varied over a wide

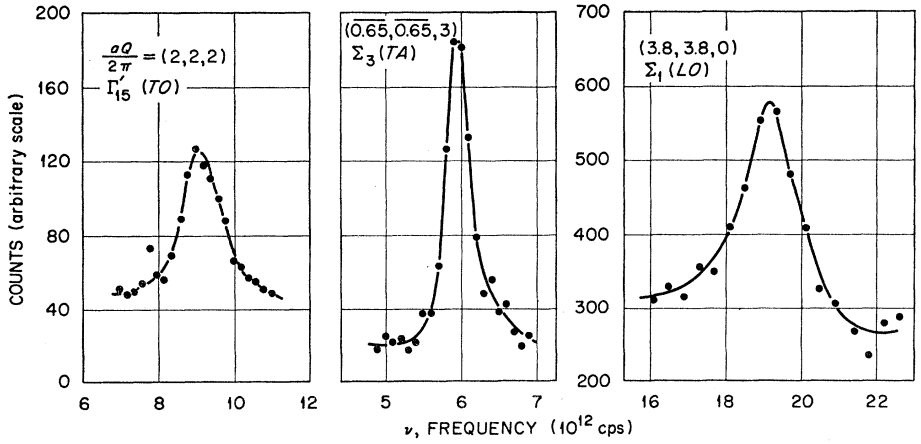

FIG. 2. Typical neutron groups observed in experiments using the "constant-Q" mode of operation. The high-frequency LO mode was measured with the High Flux Isotope Reactor (HFIR) spectrometer, while the other two scans were obtained at the ORR reactor.

[21] R. M. Nicklow, G. Gilat, H. G. Smith, L. J. Raubenheimer, and M. K. Wilkinson, Phys. Rev. **164**, 922 (1967).
[22] B. N. Brockhouse, in *Inelastic Scattering of Neutrons in Solids and Liquids* (International Atomic Energy Agency, Vienna, 1961), p. 113.

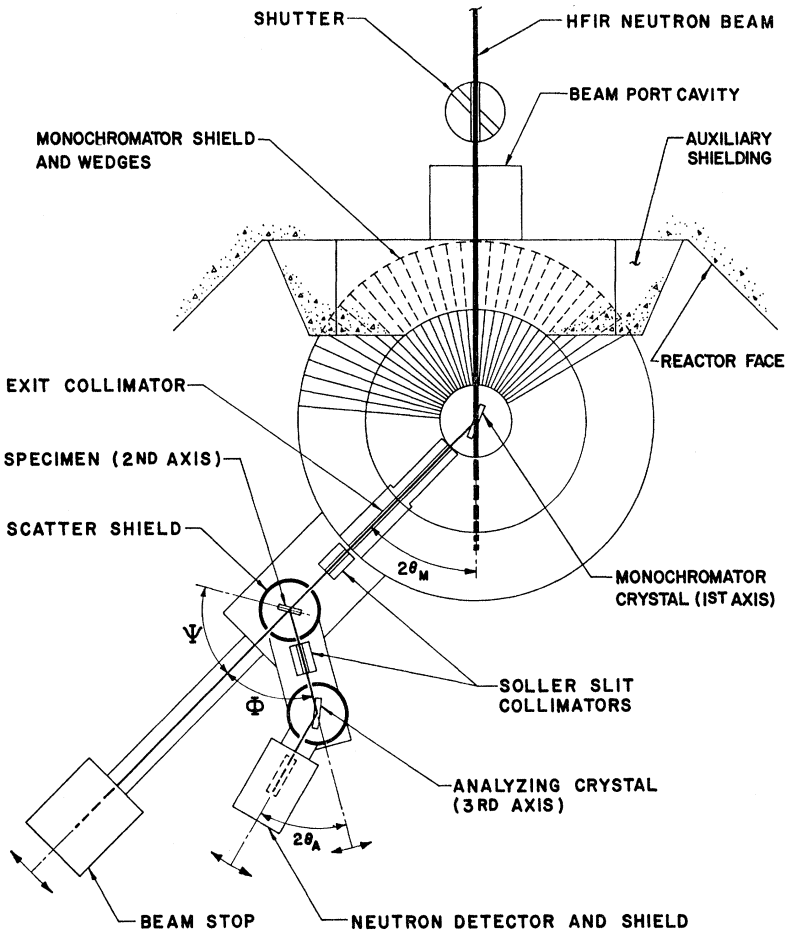

FIG. 3. Schematic diagram of the triple-axis crystal spectrometer mounted at the HFIR.

range of angle ($2\theta_M = 0$ to 90°) instead of being restricted to any one of four fixed values, and (b) the control of the spectrometer (calculation and movement of angles, recording of data, and so on) is achieved by means of a PDP-8 computer, operating on-line. In the measurement of relatively high frequencies of the LO phonons it was most convenient to utilize the (111) reflecting planes of a germanium single crystal as the analyzer of the spectrometer, in order to avoid serious problems of order contamination[23] in the scattered neutron beam. The germanium crystal used was thermally and mechanically distorted[23] to improve its reflectivity to an acceptable level.

TABLE I. A selection of measured normal-mode frequencies (units 10^{12} cps) in Li^7F at 298°K.

Γ_{15}' (LO)	19.7 ±0.25	Γ_{15}' (TO)	9.15±0.12
X_2' (LO)	13.7 ±0.20	L_1' (LO)	18.9 ±0.30
X_2' (LA)	10.5 ±0.20	L_1 (LA)	11.60±0.12
X_5' (TO)	10.35±0.20	L_3' (TO)	9.00±0.15
X_5' (TA)	7.70±0.08	L_3 (TA)	6.20±0.06

[23] G. Dolling and H. Nieman, Nucl. Instr. Methods **49**, 117 (1967).

D. Results

A selection of measured phonon frequencies in Li^7F at 298°K is given in Table I, and the complete results are shown in Fig. 4. The experimental errors are generally between 1 and 3%. The various branches of the dispersion relation have been labeled according to the characters of the irreducible representations of the appropriate wave vectors, using the tables of Koster.[24] If, alternatively, the notation of Bouckaert, Smoluchowski, and Wigner[25] is used, then X_2' and L_1' should be replaced by X_4' and L_2', respectively. The solid curves are the result of a nonlinear least-squares fit to the data on the basis of a dipole approximation model to be discussed in Sec. III.

Attempts were made to study the effect of changing the lithium isotopic composition in LiF. The mass ratio of lithium isotopes (7:6) is relatively large, but unfortunately the Li^6 isotope has a high neutron absorption cross section (950 b for 1.8 Å neutrons), and the

[24] G. F. Koster, in *Solid State Physics*, edited by F. Seitz and D. Turnbull (Academic Press Inc., New York, 1957), Vol. V, p. 173.

[25] L. P. Bouckaert, R. Smoluchowski, and E. Wigner, Phys. Rev. **50**, 58 (1936).

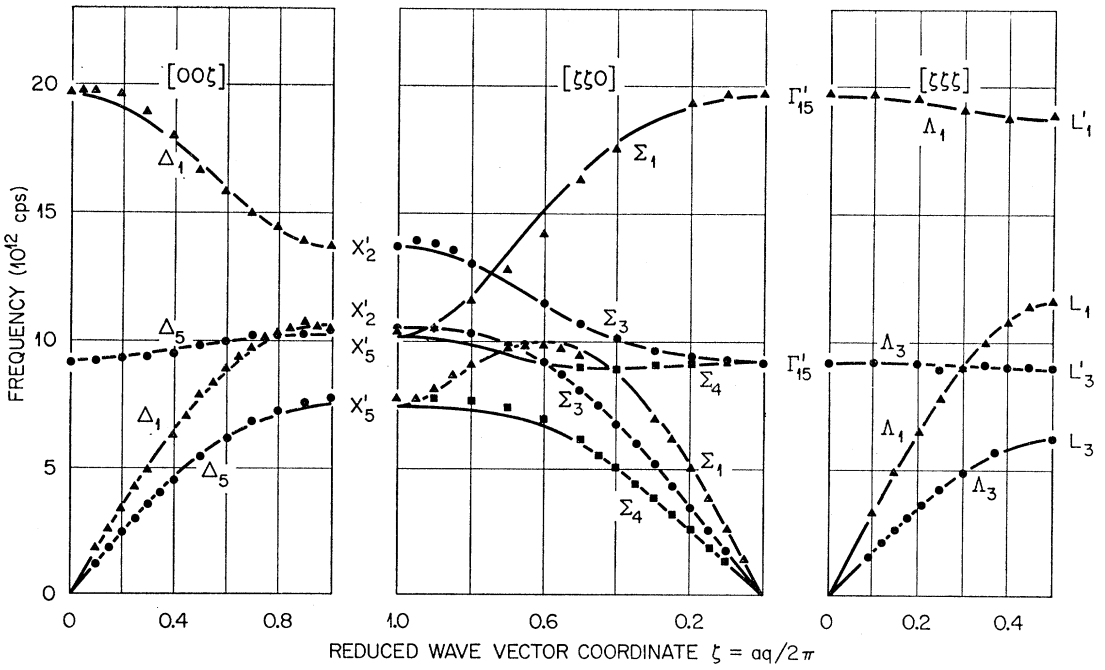

FIG. 4. Measured dispersion curves along three directions of high symmetry in Li^7F at 298°K. The solid lines are the best least-squares fit to the results on the basis of a 7-parameter dipole approximation model.

scattered neutron intensities from Li^6F or mixed Li^6-Li^7F crystals are correspondingly reduced. Preliminary results indicate that the optic mode frequencies are shifted roughly in proportion to the square root of the Li mass change, while acoustic modes are more or less unaffected.

All of the experimental results given here were obtained with 0.6° Soller-slit collimators both before and after the specimen. In addition, LA modes with reduced wave vectors $\mathbf{q}$, (0,0,0.15), (0.03,0.03,0.15), and (0,0,0.20) were observed using 0.3° Soller-slit collimators and also using 0.5° "honeycomb"-type collimators. Measurements were made for $\pm\mathbf{q}$ associated with reciprocal lattice vectors $\boldsymbol{\tau}$, (113), and ($\bar{1}\bar{1}3$), so as to provide a fairly complete picture of the shape of the dispersion relation in the vicinity of the Δ direction. The uncorrected results are given in Table II. The difficulty with making precise absolute measurements of these long-wavelength modes is that the spectrometer resolution function embraces a region of wave-vector space over which the dispersion relation varies in an anisotropic, nonlinear manner. In particular, the frequency of the LA mode (Δ_1) in Li^7F rises roughly parabolically as δ_x for wave vectors $(\delta_x,\delta_x,\zeta_z)$ slightly removed from the Δ symmetry direction. This produces a shift in the observed scattered neutron peak towards higher frequency; in contrast, wave vectors such as $(0,0\zeta_z\pm\delta_z)$ give rise to small downward peak shifts owing to the frequency dependence of the neutron-scattering cross section. In principle, these effects may be calculated by convoluting the spectrometer resolution function (specified by instrumental parameters such as crystal mosaic spreads, collimator transmission functions, etc.) with the behavior of $\nu(\mathbf{q})$ in the region appropriate to the measurement. The latter can be computed from a theoretical interatomic force model based on approximately corrected results. Alternatively, we may attempt to deduce the corrected value of the phonon frequency for a wave vector $(0,0,\zeta_z)$ from experimental observations in its vicinity as outlined above. In this latter way we have deduced corrected values for $\zeta_z=0.15$ and 0.20, which are shown in Table II together with the values which would be expected from the known isothermal elastic constant C_{11}, assuming a linear dispersion relation and neglecting anharmonic effects. It should be noted that the instrumental corrections to the observed frequencies are rather large; in spite of this, however, there still remains a substantial discrepancy between the experimentally determined phonon frequency and that which

TABLE II. Frequencies of $\Delta_1 A$ modes (units 10^{12} cps) for low $\mathbf{q}$ values, compared with those expected from the isothermal electric constant C_{11}. The measurements were made with 0.3° Soller-slit collimators before and after the specimen. The corrected frequencies which would be obtained in the absence of normal-mode dispersion effects are listed as ν_L.

$(a/2\pi)\mathbf{q}$			ν(uncorr.)	ν(corr.)	ν_L	ν (from C_{11})
0.03	0.03	0.15	2.68±0.04			
0	0	0.15	2.61±0.03$_5$	2.52±0.06	2.55	2.41
0	0	0.20	3.34±0.04$_5$	3.26±0.07	3.32	3.21

TABLE III. Parameters of three dipole approximation models for the lattice dynamics of Li^7F. All the short-range force constants are quoted in units of $(e^2/2v)$, where v is the volume of the primitive unit cell.

Model parameters	Units	I	II	III
A	$e^2/2v$	7.739	6.797	7.503
B	$e^2/2v$	−0.874	−0.653	−0.827
A'	$e^2/2v$	−0.317	···	···
B'	$e^2/2v$	0.051	···	···
A''	$e^2/2v$	1.030	1.048	1.066
B''	$e^2/2v$	−0.056	−0.049	−0.070
Z	e	0.970	0.902	0.950
α_1	$1/v$	0.0062	···	···
d_1	e	−0.0270	···	···
α_2	$1/v$	0.0447	0.0420	0.0485
d_2	e	0.1460	0.1083	0.1342
χ		1.53	1.55	1.45

would be expected from the elastic constant C_{11} (isothermal or adiabatic) at 300°K.[26] The elastic constants of LiF (usually natural LiF rather than Li^7F, but the differences between these would be expected to be very slight) have been measured on several occasions[26] and there are serious inconsistencies in these data. Although further remeasurement of the elastic constants as a function of temperature would be desirable to resolve these disagreements, it seems likely that C_{11} at 300°K is less than 11.5×10^{11} dyn/cm², substantially less than the value derived from our measurements of the LA (Δ) phonons. We have also computed C_{11} from the best-fit dipole approximation models to be described in Sec. III; the result is in the range 11.8 to 12.8($\times10^{11}$ dyn/cm²) depending on the exact details of the model used. Further neutron-scattering experiments on Li^7F, using an even finer collimation system and also varying the temperature, are being planned in order to investigate these effects in more detail. The results will be given in a future publication.

III. THEORETICAL CALCULATIONS

A. Models

A substantial literature now exists on the subject of interatomic force models for alkali halide crystals (see Ref. 3 for a review). As is well known, it is important to take into account not only the short-range "overlap repulsion" forces between near-neighbor ions, and the Coulomb forces between their positive and negative charges, but also the electrostatic forces which arise because of distortions of the electronic configurations of the ions due to the passage of lattice waves. These distortions can be treated as an electric multipole expansion about the ion sites. Cutting off this series after the dipole term leads to the dipole approximation model or "shell" model proposed originally by Dick and Overhauser.[27] The most general form of this model involves a very large number of adjustable parameters, and several different simplifying assumptions have been used in the past to reduce this number. Here, we shall adopt the approximations[4,11] that the short-range forces act entirely through the outer valence electrons (the "shells"), and that the overlap forces are axially symmetric[28] and extend to, at most, second-nearest-neighbor ions. The most general model we have considered (model I) is thus specified by 11 parameters: radial and tangential short-range force constants A, B, A', B', A'', B'', between Li^+-F^-, Li^+-Li^+, and F^--F^- near-neighbor ions, respectively, the ionic charge Ze, and the electrical and mechanical polarizabilities α_1, d_1, α_2, d_2, for the Li^+ and F^- ions, respectively. In model II, the Li-Li forces and Li^+ polarizibilities (A', B', α_1, d_1) are set equal to zero, in recognition of the fact that the Li^+ is a very small and tightly bound ion. The notation used is described in detail elsewhere.[29] Several other variations of this basic model were also tried; for example, models with Z kept fixed at 1.0. Application of the condition for central forces[4] led to generally less satisfactory fits to the experimental results, mainly because this condition implies the Cauchy relation $C_{12}=C_{44}$ which is definitely not obeyed by LiF. The actual discrepancy is probably due to many-body forces, as discussed by Löwdin[12] and Lundquist.[13] To take these effects into account in a proper and satisfactory manner would seem to be an extremely difficult problem. Clearly, the relaxation of the equilibrium condition, and hence the Cauchy relation, represents in a crude way the many-body effects. Regarded as a purely phenomenological device to improve the fit to the results, this would seem to be as useful an approach as any, at least until the appropriate many-body calculations can be performed. As stated earlier, the results have also been analyzed in terms of the breathing shell model (BSM).[14,15] This is a modification of the Cochran shell model in which a new coordinate expressing the compression of the electron shells is introduced, in addition to the ionic displacements and dipole moment coordinates. The necessity of additional parameters representing, in some sense, the shell compressibilities, is conveniently avoided, following Nusslein and Schröder, by equating these to the spring constants (k_1, k_2 in Cochran's notation; G_1, G_2 in Ref. 15) describing the force between a core and its shell. The justification for this procedure is somewhat obscure; one might imagine that the shell compressibility would depend on the complicated interactions between the electrons comprising the shell, and that compression of a shell might affect the appropriate k value. Neither of these physical effects is directly represented in the BSM. Viewed in this light, the BSM is merely another in a long line of phenomeno-

[26] R. A. Miller and C. S. Smith, J. Phys. Chem. Solids **25**, 1279 (1964); C. V. Briscoe and C. F. Squire, Phys. Rev. **106**, 1175 (1957); K. Spangenberg and S. Haussühl, Z. Krist. **109**, 422 (1957).

[27] B. G. Dick and A. W. Overhauser, Phys. Rev. **112**, 90 (1958).

[28] T. Wolfram, G. W. Lehman, and R. E. De Wames, Phys. Rev. **129**, 2483 (1963).

logical variations of the basic shell model. It is nevertheless of interest to test the usefulness of this variant as a faithful description of experimental data, and to compare it with the analogous Cochran shell model. Accordingly, a seven-parameter model (called model III) was constructed from model II by allowing the F^- shell to "breathe" in the manner prescribed by Nusslein and Schröder. Our model III differs from theirs only in that the ionic charge is allowed to vary instead of being fixed at 1.0.

Having decided upon the details of a particular force model, we obtained the best values of the model parameters by means of a nonlinear least-squares fitting program written for the CDC-1604 computer at the Oak Ridge National Laboratory. The results of this process for models I, II, and III, mentioned above, are shown in Table III and in Fig. 4 (the solid curves are for model II). Although model I actually gave a very slightly better fit than model II to the results, it is clear from Fig. 4 that model II, in which Li-Li short-range forces and the Li^+ polarizability are neglected, provides an excellent fit to the neutron-scattering results. Model III, the "breathing" shell model, gave a slightly better fit still to the results, although the calculated dispersion curves for all three models would be virtually indistinguishable if plotted in Fig. 4. (The differences are, indeed, statistically insignificent.) It is perhaps interesting to note that models II and III provide an identical "quality-of-fit" number (χ) for the phonon frequencies alone; however, the BSM seems to fit the dielectric constants rather better than model II, and this accounts for all the discrepancy in χ noted in Table III. Attempts to force the models to fit both neutron data and isothermal elastic constants simultaneously were unsuccessful, and we suggest that this implies a real discrepancy, arising from anharmonic effects,[17] between phonon frequency measurements made in the high (10^{12}-cps) and low (10^9-cps) frequency regimes. The squared ratio of the measured LO and TO mode frequencies for very small wave vectors is 4.63 ± 0.16, as compared with 4.53 ± 0.2 for the ratio of the low- and high-frequency dielectric constants ($\epsilon_0/\epsilon_\infty$). The Lyddane-Sachs-Teller relation[30] is thus seen to be valid for Li^7F, well within experimental error.

B. Calculations from Models

Since all three models discussed above gave essentially identical fits to the phonon frequencies, it seemed unnecessary to perform the following calculations with more than one of them, and model II was selected for this purpose:

(a) Inelastic structure factor: This has been discussed in Sec. II A. The results of a calculation of g_j^2 are plotted in Fig. 5, in units of $[(\hat{\xi}_j\cdot\mathbf{Q}b_1)^2/(m_1\nu_j)]$. These

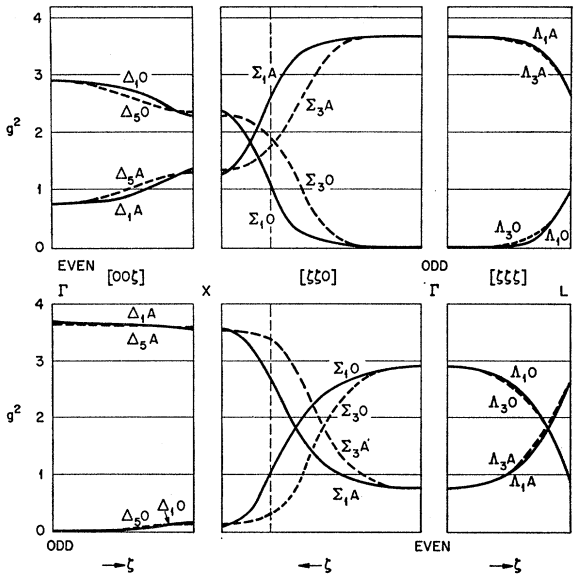

FIG. 5. Reduced inelastic structure factor curves for various branches of the phonon spectrum, calculated on the basis of model II.

curves show significant differences from the analogous curves [4] for NaI, not only because of the different interatomic forces involved, but also because of the negative scattering length of Li^7 ($b=-0.21\times10^{-12}$ cm).

(b) Frequency distribution function: This has been computed by the numerical root-sampling program of Gilat and Raubenheimer,[31] appropriately modified for the case of the LiF crystal structure. The frequencies, eigenvectors, and frequency gradients are computed for a number (in our case 977) of reduced wave vectors $\mathbf{q}_c$ distributed in three subsections within the irreducible 1/48 of the Brillouin zone. The spacing between neighboring $\mathbf{q}_c$ values is ζ. Assuming the gradients to be constant over the volume of a small cube of side ζ, surrounding a given $\mathbf{q}_c$, we calculate the area of each constant frequency surface (frequency ν to $\nu+\Delta\nu$) intersecting the cube, and this is directly proportional to the contribution of the mode to the frequency distribution $g(\nu)\Delta\nu$. Summing over all modes and all cubes needed to fill the Brillouin zone, we arrive at a very accurate representation of the function $g(\nu)$, as shown in Fig. 6(a). In this histogram plot, the frequency channel width is 0.01×10^{12} cps, and so the points are too close together to be plotted individually. The locations of several critical points[16] are clearly shown, and may be correlated with appropriate features of the dispersion curves in the principal symmetry directions as shown in Fig. 4. The other critical points are associated with zero-gradient regions of dispersion curves in unmeasured symmetry directions (such as Q, S, and Z) and in off-symmetry directions.

(c) Debye-Waller factors: The Debye-Waller factor

[29] W. Cochran, R. A. Cowley, G. Dolling, and M. M. Elcombe, Proc. Roy. Soc. (London) A293, 433 (1966).
[30] R. H. Lyddane, R. G. Sachs, and E. Teller, Phys. Rev. 59, 673 (1941).
[31] G. Gilat and L. J. Raubenheimer, Phys. Rev. 144, 390 (1966).

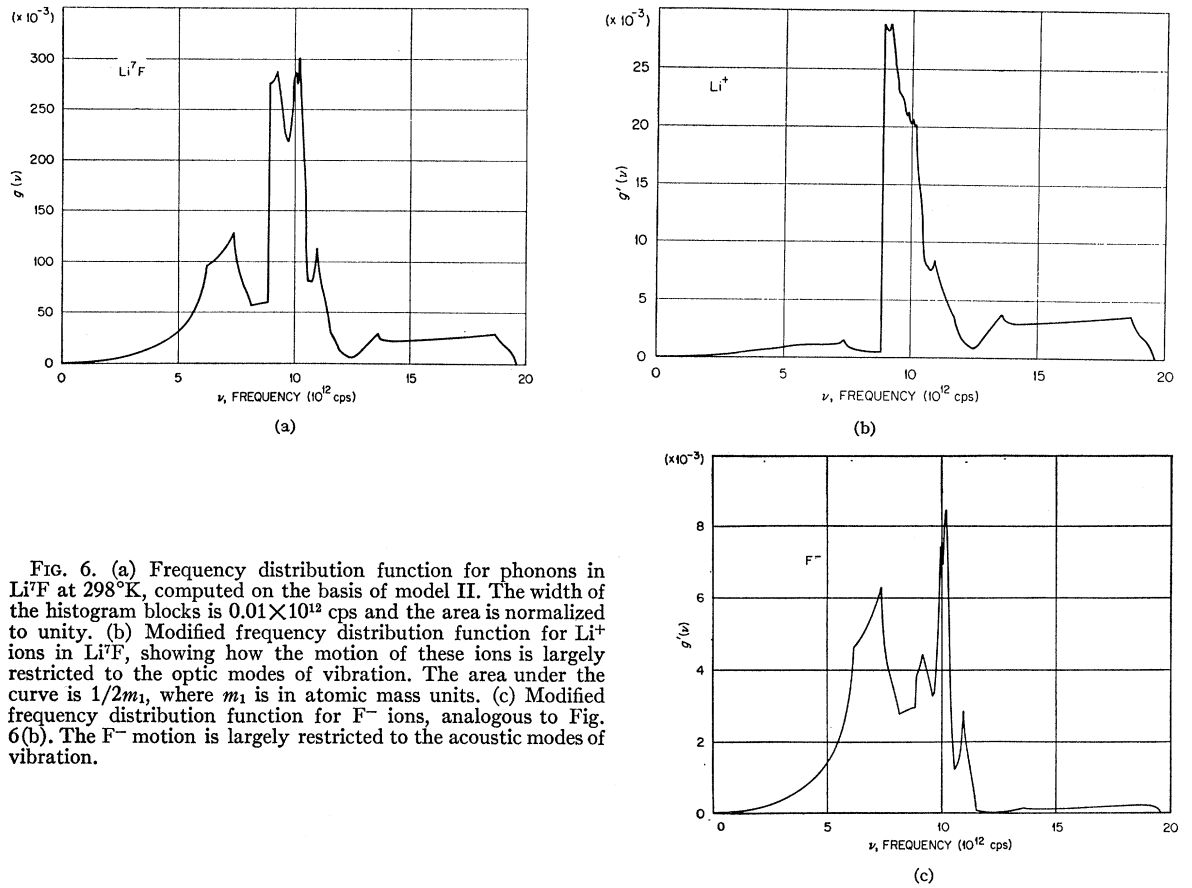

FIG. 6. (a) Frequency distribution function for phonons in Li^7F at 298°K, computed on the basis of model II. The width of the histogram blocks is 0.01×10^{12} cps and the area is normalized to unity. (b) Modified frequency distribution function for Li^+ ions in Li^7F, showing how the motion of these ions is largely restricted to the optic modes of vibration. The area under the curve is $1/2m_1$, where m_1 is in atomic mass units. (c) Modified frequency distribution function for F^- ions, analogous to Fig. 6(b). The F^- motion is largely restricted to the acoustic modes of vibration.

$\exp(-W_s)$ for the sth ion, where $W_s=|\mathbf{Q}|^2B_s$ (for the LiF structure) and

$$B_s=(\hbar/24\pi N)\sum_{qj}\coth(h\nu_j/2k_BT)\,|U_{sj}|^2/\nu_j,$$

can be computed from the eigenvectors of the normal modes, as given by model II, for example. First, we compute two modified distribution functions $g_1(\nu)$ and $g_2(\nu)$, for the Li^+ and F^- ions, respectively: As each normal mode frequency is calculated, it is weighted by the square of the appropriate Li^+ or F^- eigenvector and stored in histogram form in the same way as $g(\nu)$ itself. Values of W_s are subsequently evaluated at several temperatures by suitably summing over the functions $g_s(\nu)$. These functions (obtained from model II) are shown in Figs. 6(b), 6(c), and the derived mean-square ionic displacements are shown in Fig. 7. The horizontal region of the curves at low temperature is given by the zero-point vibration amplitudes. Comparison of curves 6(b) and 6(c) shows that the acoustic modes involve the motion mainly of the F^- ion, with very little contribution from Li^+, and vice versa for the optic modes.

(d) Heat capacity and Debye temperature: These may be readily computed in the harmonic approximation from the frequency distribution function $g(\nu)$. Since anharmonic effects have been neglected, it is perhaps surprising that the model provides such a good fit to the experimentally measured heat capacity,[32–34] as displayed in terms of the Debye temperature parameter (Fig. 8). Indeed, it seems that the room-temperature phonon frequencies (as represented by the force models) are numerically in better accord with the low-temperature elastic constants, and hence the low-temperature calorimetric data, than with their room-temperature values. The various measurements of the heat capacity (as represented by the dashed curve of Fig. 8) are in good agreement except for temperatures below about 25°K. The low-temperature limits of θ_D display discrepancies of 1–2%, but these are certainly smaller than the probable error in the calculated value (723°K). We have also calculated the entropy of Li^7F from model II, again in the harmonic approximation; the equivalent Debye temperature Θ_S derived from this is also shown in Fig. 8.

C. Optical Properties

Optical properties of alkali halide and other types of host crystals containing charged defects have been

[32] D. L. Martin, Phil. Mag. **46**, 751 (1955).
[33] K. Clusius and W. Eichenauer, Z. Naturwiss. **11a**, 715 (1956).
[34] W. W. Scales, Phys. Rev. **112**, 49 (1958).

widely studied in recent years.[35–39] The zero-phonon absorption lines, which arise from purely electronic transitions, may display more or less complex sidebands, corresponding to the emission of one or more phonons in conjunction with the electronic transition. If the symmetries of the defect and of the electronic levels are known, then group-theoretical arguments can be used to deduce selection rules[40] governing which phonons may take part in these phonon-assisted transitions. In the case of lithium fluoride, attempts have been made to identify certain peaks in these sideband spectra with particular phonons, using the calculated dispersion curves of Karo and Hardy[10] as a guide in making the assignments. However, the majority of the assignments made so far are probably incorrect, partly because their calculated[10] normal mode frequencies of LiF are only roughly (10–20%) in agreement with our experimental values, and partly because the above-mentioned symmetry arguments have not been properly applied. For example, Pierce[35] observes two well-defined sets of peaks corresponding to phonon frequencies 6.17 and 7.58 ($\times 10^{12}$ cps), and assigns these to the X_5' and L_3' modes, respectively (see Fig. 4). These values refer to very low temperatures, whereas our neutron-scattering results were obtained at room temperature. We estimate that the average change in frequency due to the temperature dependence of the normal modes is less than 5%. In spite of this uncertainty (which could be removed by appropriate low-temperature neutron-scattering experiments), it is clear that these assignments are incorrect, and should probably be L_3 and X_5', respectively. In the same way, many of the assignments made by Fitchen[37] and by Hughes[39] need to be revised in view of our results. In some cases, such as the peak E observed by Hughes, it is not at present possible to obtain an unambiguous assignment since several critical-point frequencies are very close together in this region, and all may contribute to the sideband absorption. However, in most cases, the distribution function of Fig. 6(a), together with the calculated normal-mode frequencies for all the major symmetry points, as listed in Table IV, and the measured frequencies of Table I, can provide a useful guide in the interpretation of these optical properties.

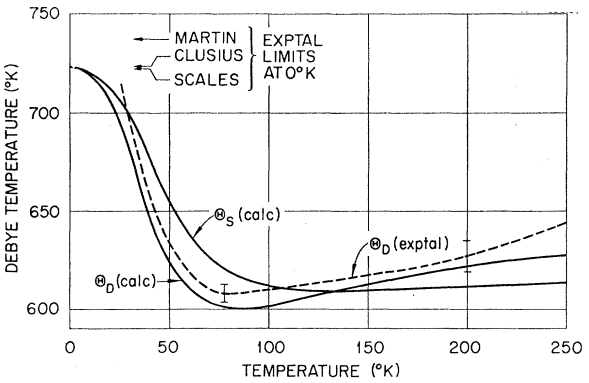

FIG. 8. Temperature dependence of the Debye temperature of LiF, derived from experimental measurements (see Refs. 32–34) of the heat capacity and from the heat capacity (Θ_D) and entropy (Θ_S) calculated from model II.

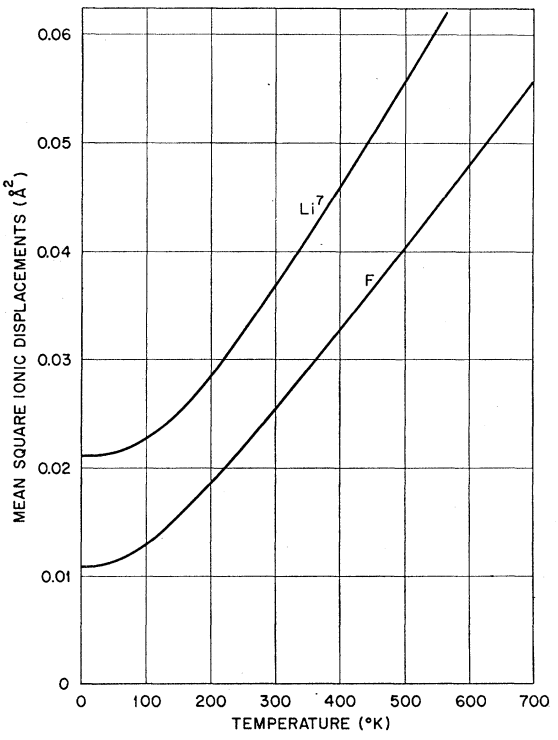

FIG. 7. Mean square ionic displacements for Li^+ and F^- ions derived from Figs. 6(b) and 6(c).

We have also calculated combined density of states functions for Li^7F from model II. At each $\mathbf{q}$ in the Brillouin zone, each of the six normal-mode frequencies is added to the other frequencies in turn (both including and excluding itself) and the resultant two-phonon sum frequencies are sorted into histogram plots. An extrapolation method analogous to that of Ref. 31 was employed to obtain very high-frequency resolution for these distributions. As expected, these show many critical points and other singular features, and are useful

TABLE IV. Frequencies (units 10^{12} cps) of normal modes at high-symmetry points, calculated from model II.

Γ_{15}' 19.58; 9.20	L_1' 18.69
X_2' 13.62; 10.54	L_1 11.50
X_5' 10.18; 7.39	L_3' 8.85
W_3 11.80; 9.59	W_2' 11.37
	W_1 8.13

[35] C. B. Pierce, Phys. Rev. **135**, A83 (1964).
[36] M. Wagner and W. E. Bron, Phys. Rev. **139**, A223 (1965).
[37] D. B. Fitchen (private communication).
[38] D. B. Fitchen, R. H. Silsbee, T. A. Fulton, and E. L. Wolfe, Phys. Rev. Letters **11**, 275 (1963).
[39] A. E. Hughes, Proc. Phys. Soc. (London) **88**, 449 (1966).
[40] R. Loudon, Proc. Phys. Soc. (London) **84**, 379 (1964).

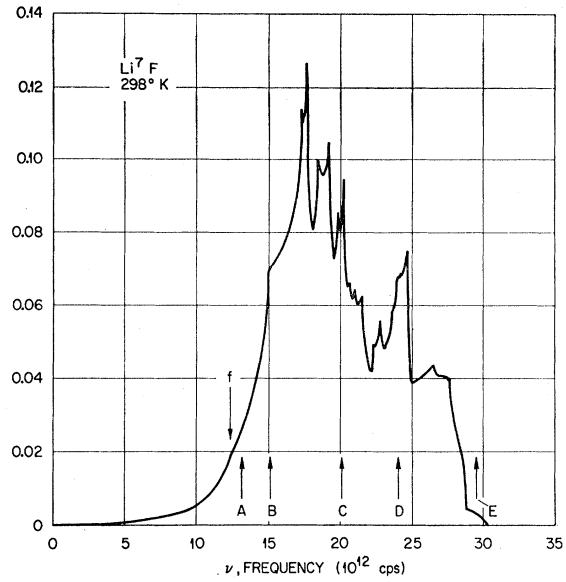

FIG. 9. Combined density of states function for Li^7F at 298°K. Only summation bands and combination bands (no overtones) are included. The arrows indicate certain singular features observed (see Ref. 41) in the infrared absorption spectrum of LiF at 90°K.

for interpreting such properties as two-phonon infrared absorption spectra and second-order Raman spectra for Li^7F.

In Fig. 9 is shown the combined density-of-states function for Li^7F obtained when only summation and combination bands are included. Difference bands $[\nu_j(\mathbf{q})-\nu_{j'}(\mathbf{q})]$ and overtones $[\nu_j(\mathbf{q})\pm\nu_{j'}(\mathbf{q})$ for $j=j']$ are omitted since these are inappropriate for the purposes of comparison with the infrared absorption measurements[41] at 90°K. The width of the histogram blocks is 0.02×10^{12} cps. Even though overtones are omitted, and hence critical points such as L_3+L_3 [or 2TA(L)] should not appear in Fig. 9, there is an indication of this critical point at $\nu=2\times6.20=12.40\times10^{12}$ cps. This arises because in the region of reciprocal space close to L, these two modes are not quite degenerate, and their combination is not forbidden by symmetry. In practice, one would expect that the matrix elements for infrared absorption involving these very close pairs of modes would be very small and the absorption unobservable. Thus the distribution of Fig. 9 may display rather more critical points and other singular features than would be observed experimentally. In addition, we must bear in mind that it is a model calculation based on room-temperature data, and so one might expect $\approx5\%$ discrepancies between the experimental and calculated locations of critical points. Nevertheless, from a consideration of Table IV and Fig. 9, the following conclusions may be drawn:

(a) The observed feature A has no matching feature at all in the computed distribution. Its frequency is much lower than the lowest possible combination critical point, if only sums of frequencies are considered.

(b) Feature B might be explained in terms of combinations in the vicinity of the L_3+L_3' combination, although the above discussion indicates that the appropriate matrix elements would be small.

(c) Feature C could correspond with any or all of three combinations $W_2'+W_3$, $X_2'(A)+X_5'(0)$ or $X_2'(0)+X_5'(A)$.

(d) Feature D could correspond with any of five possible combinations $\Sigma_1(0)+\Sigma_4(A)$, $\Sigma_1(0)+\Sigma_3(A)$, W_3+W_2', $X_2'(0)+X_5'(0)$, $X_2'(A)+X_2'(0)$.

(e) Feature E can be explained in terms of an $L_1'+L_3'$ combination if these modes have frequencies about 6% higher at 90°K than at 298°K. If this change is typical for all the modes, then it becomes even more difficult to understand the origin of features A and B.

IV. SUMMARY

Dispersion curves for the normal modes of vibration of Li^7F have been measured at 298°K. These results are well fitted by a 7-parameter dipole approximation model involving nearest-neighbor and second-nearest-neighbor F^--F^- short-range forces, a variable ionic charge, and the polarizability of the F^- ions only. Modification of this model according to the prescription of Schröder[14] produces no improvement in the fit to the phonon frequencies. Certain inconsistencies have been found between the slopes of acoustic branches near $\mathbf{q}=0$ and the appropriate velocities of sound as measured by ultrasonic techniques. It is believed that these arise from anharmonic effects.[17]

The best-fit dipole approximation model has been used to compute various other properties of LiF in a pseudoharmonic approximation. Of particular interest are the comparisons which can be made between the calculated phonon density of states and combined density-of-states functions and appropriate experimental measurements of optical and infrared absorption in this material.

It is evident, however, from the previous discussion that further neutron-scattering experiments on lithium fluoride at various (lower) temperatures would be most valuable, and such experiments are planned for the near future. It is also hoped to carry out experiments on Li^6F, and on mixed Li^6F-Li^7F crystals, to study in detail the effects of changing the ionic mass without affecting the interionic forces. Finally, we intend to make a more detailed study of the frequencies of long-wavelength acoustic modes, as mentioned in Sec. II D.

[41] A. M. Karo, J. R. Hardy, C. Smart, and G. R. Wilkinson, in *Lattice Dynamics*, edited by R. F. Wallis (Pergamon Press Inc., New York, 1965), p. 387.